Supporting Information

Tunable Afterglow Luminescence and Triple-mode Emissions of Thermally Activated Carbon Dots Confined within Nanoclay

Yuchen Deng, Peng Li, Haiyan Jiang, Xu Ji and Huanrong Li**

National-Local Joint Engineering Laboratory for Energy Conservation in Chemical Process Integration and Resources Utilization, Tianjin Key Laboratory of Chemical Process Safety, School of Chemical Engineering and Technology, Hebei University of Technology, GuangRong Dao 8, Hongqiao District, Tianjin 300130, P. R. China.

E-mail: lihuanrong@hebut.edu.cn.

Materials and Methods

The layered clay (Laponite® RD) was purchased from Rockwood Additives Ltd. Pyridine-2,6-dicarboxylic acid (DPA), 2,4-pyridinedicarboxylic acid, 2,5-pyridinedicarboxylic acid, 3,4-pyridinedicarboxylic acid, 3,5-pyridinedicarboxylic acid, isophthalic acid, 2,2'-Bipyridine and propionic acid were purchased from J&K Scientific Ltd and were used as received. Sodium bicarbonate ($NaHCO_3$) were obtained from Tianjin Chemical Reagent Co.

Preparation of $(DPA)_n$@clay:

Laponite® (1.0 g) was dispersed in distilled water (10 mL) and was sonicated for 10 min to obtain a transparent colloidal suspension solution. A wet gel was obtained after centrifugating and washing with distilled water for two times. Subsequently, DPA (0.2 g) was dissolved in 20 mL distilled water with a moderate amount of $NaHCO_3$ to adjust the pH to 7-8. Then $(DPA)_n$@clay nanocomponents were obtained through centrifugating, washing and drying processes.[1, 2]

Preparation of CDs@clay:

The as-prepared $(DPA)_n$@clay were placed into a muffle furnace and annealed at 550 °C for 2 h in air. The final product was donated as CDs@clay.

Preparation of CDs-1@clay ~ CDs-6@clay:

The preparation process was similar to CDs@clay. But the guest molecules were instead by 2,4-pyridinedicarboxylic acid, 2,5-pyridinedicarboxylic acid, 3,4-pyridinedicarboxylic acid, 3,5-pyridinedicarboxylic acid, isophthalic acid and 2,2'-Bipyridine. The above products were placed into a muffle furnace and annealed at 550 °C for 2 h in air. The final products were donated as CDs-1@clay ~ CDs-6@clay, respectively.

Physical measurements:

The steady-state fluorescence/afterglow spectra and afterglow decay curves were measured on an Edinburgh FLSP920 fluorescence spectrophotometer equipped with a xenon arc lamp (Xe900) and a microsecond flash-lamp (F900), respectively. The luminescent photos and videos were taken by a Canon PowerShot SX540 HS camera at room temperature. X-Ray diffraction data were recorded on a Bruker D8 diffractometer with Cu-Ka radiation. X-ray photoelectron spectroscopy (XPS) was carried out on Perkin Elmzr PHI-1600 spectrometer. Transmission electron microscopy (TEM) observations were performed on a Tecnai G2 F20 microscope. ^{29}Si solid-state NMR spectrum was recorded on Agilent 600 MHz DD2 spectrometer operating at 600 MHz.

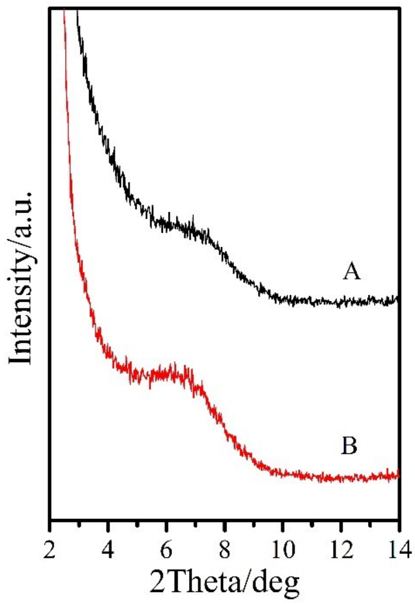

Figure S1. XRD patterns of A) the pristine clay, B) $(DPA)_n$@clay.

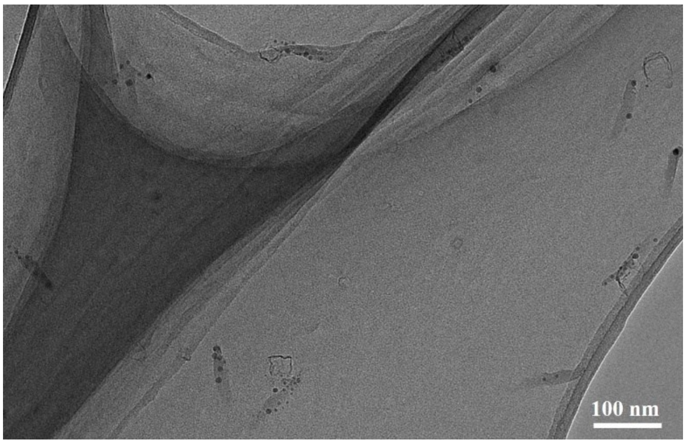

Figure S2. TEM image of CDs@clay.

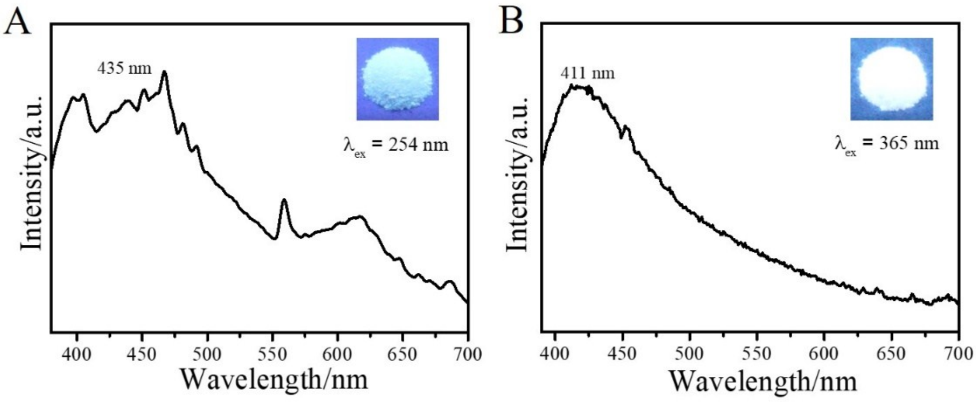

Figure S3. Fluorescence emission spectra of CDs@clay excited at A) 254 nm and B) 365 nm. Inset: Digital photographs of CDs@clay under UV light.

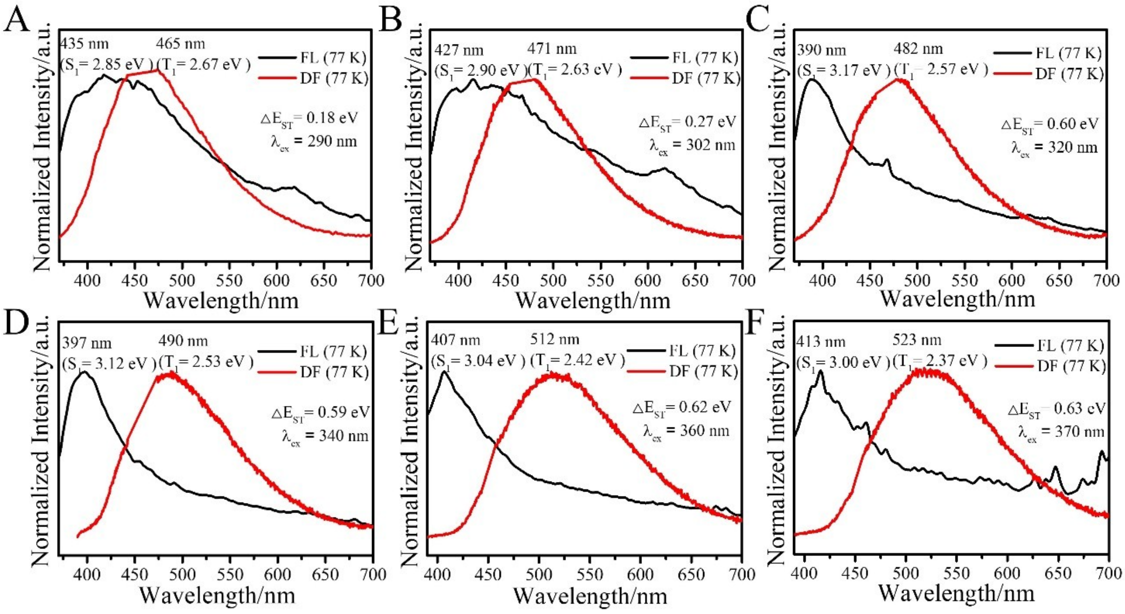

Figure S4. Normalized FL and DF/RTP emission spectra of the CDs@clay at low temperature (77 K) under excitation at A) 290 nm, B) 302 nm, C) 320 nm, D) 340 nm, E) 360 nm and F) 370 nm.

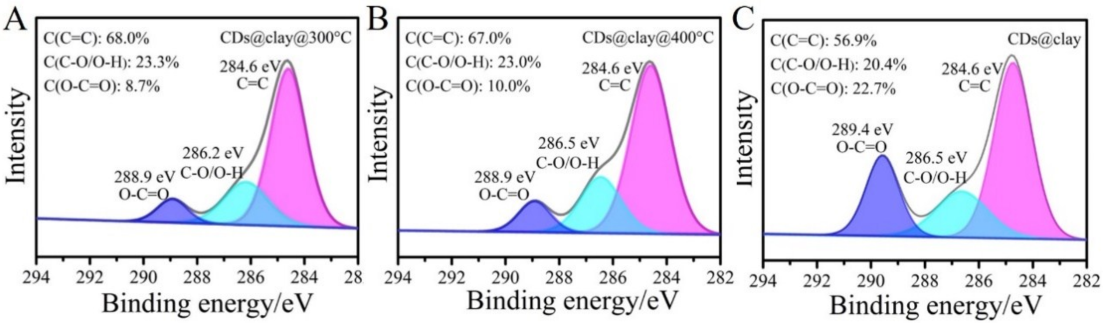

Figure S5. High-resolution XPS fitting results for the C 1s spectra of A) CDs@clay@300 ℃, B) CDs@clay@400 ℃ and C) CDs@clay.

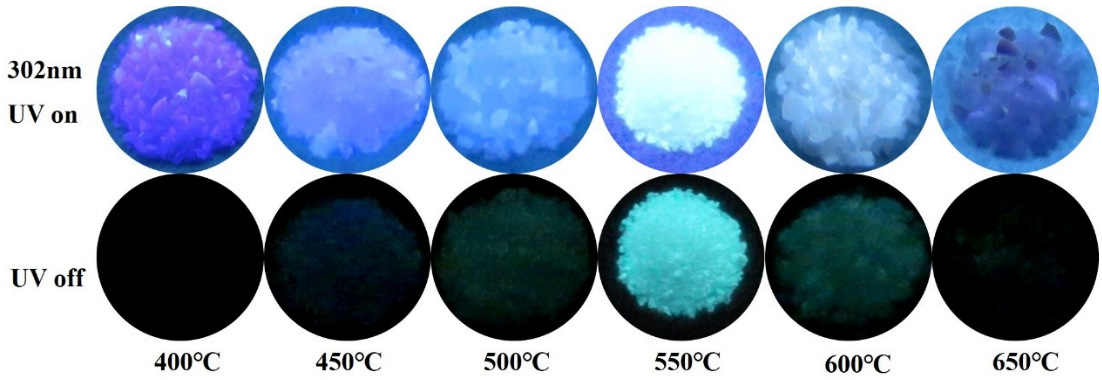

Figure S6. Digital photographs of $(DPA)_n$@clay after thermal-treatment at different temperatures before and after turning off the UV excitation under 302 nm.

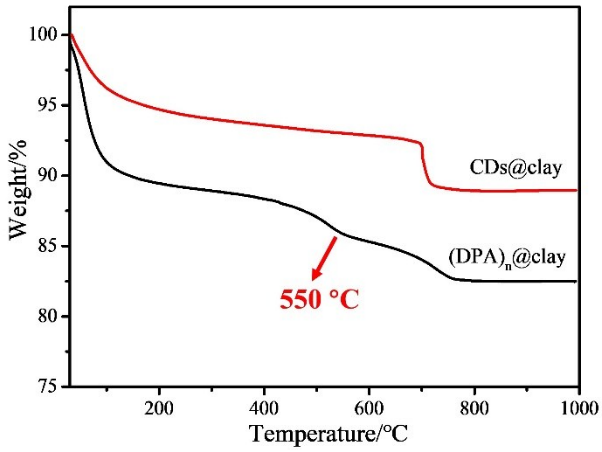

Figure S7. TGA curves of $(DPA)_n$@clay and CDs@clay.

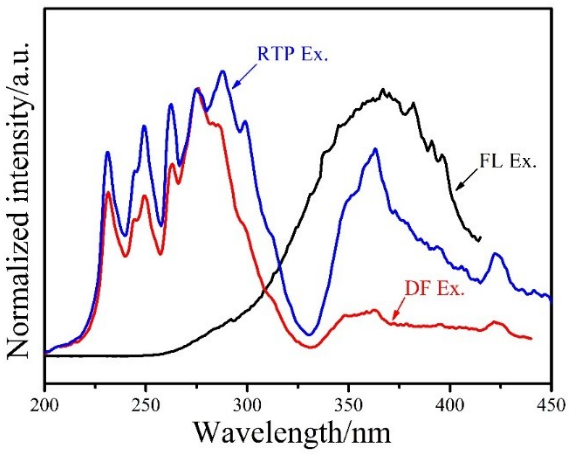

Figure S8. FL excitation spectrum (black), DF excitation spectrum (red), and RTP excitation spectrum (blue) of CDs@clay. All measurements were performed at room temperature.

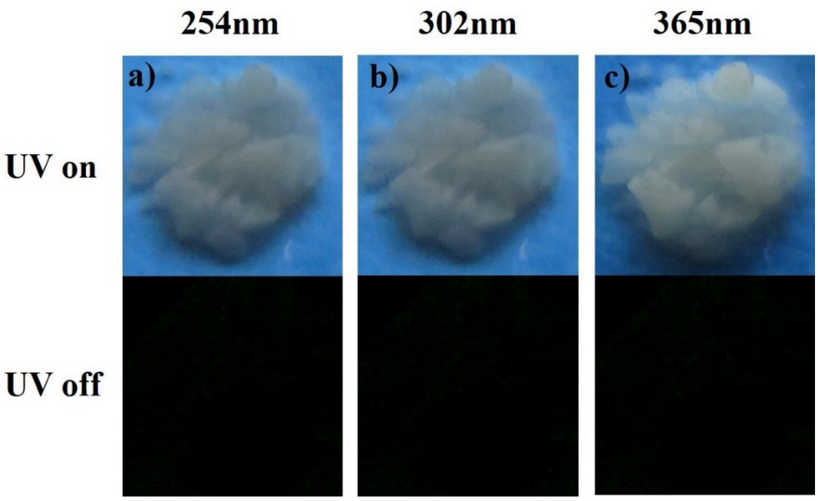

Figure 9. Digital photographs of (propionic acid)$_n$@clay before and after turning off the UV excitation of a) 254 nm, b) 302 nm, c) 365 nm.

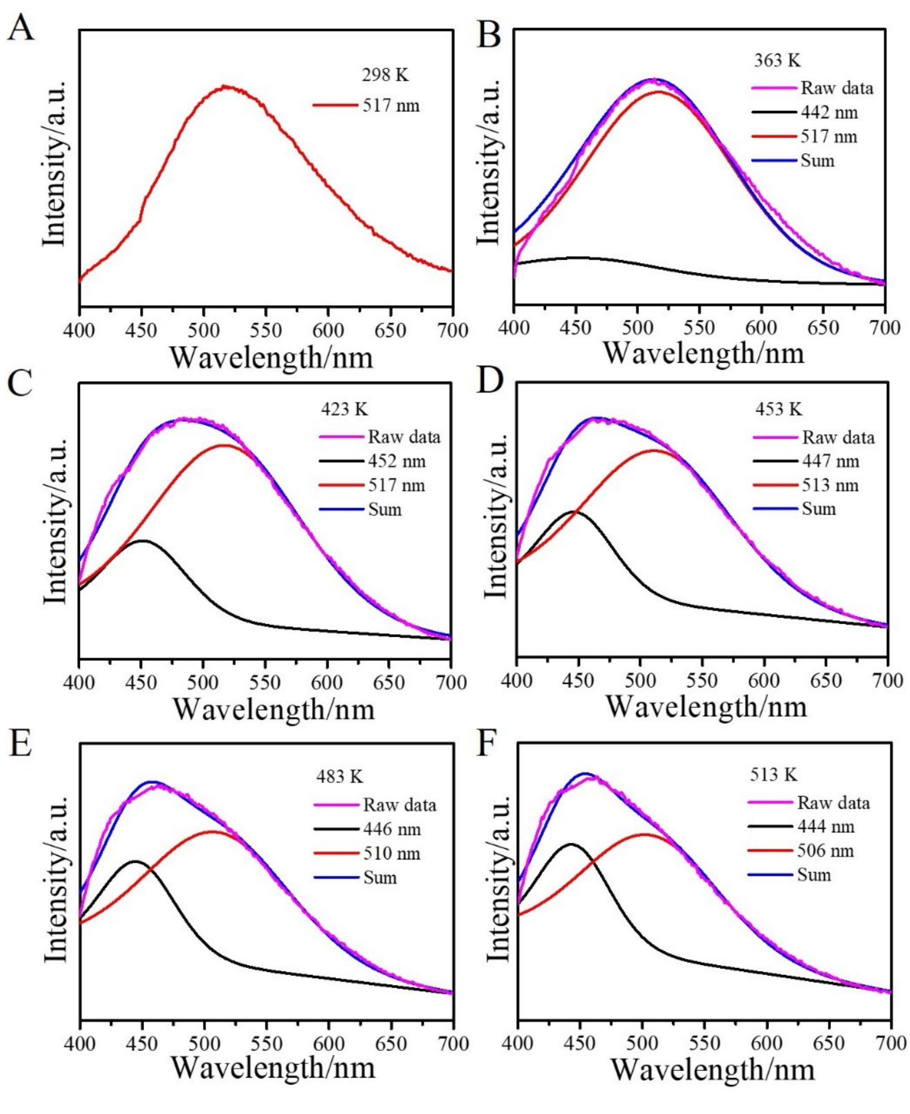

Figure S10. A-F) The afterglow emission spectra of CDs@clay at different temperatures and the Gaussian fitted by two emission peaks.

Table S1. The relative contents of the two peaks for the CDs@clay.

T [K]	λ_{em}[nm]	B_1[%]	λ'_{em}[nm]	B_2[%]
298	-	-	517	100
363	442	9.80	517	90.20
423	452	19.49	517	80.51
453	447	21.26	513	78.74
483	446	26.85	510	73.51
513	444	30.24	506	69.76

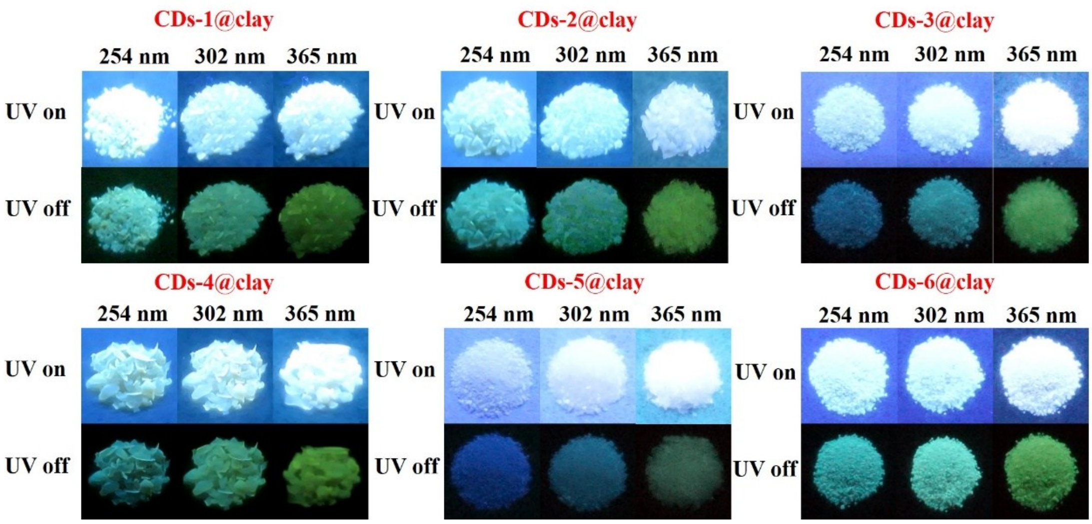

Figure S11. Digital photographs of CDs-1@clay ~ CDs-6@clay (2,4-pyridinedicarboxylic acid, 2,5-pyridinedicarboxylic acid, 3,4-pyridinedicarboxylic acid 3,5-pyridinedicarboxylic acid, isophthalic acid and 2,2'-Bipyridine as guest molecules, respectively) before and after turning off the UV excitation under ambient conditions and air atmosphere.

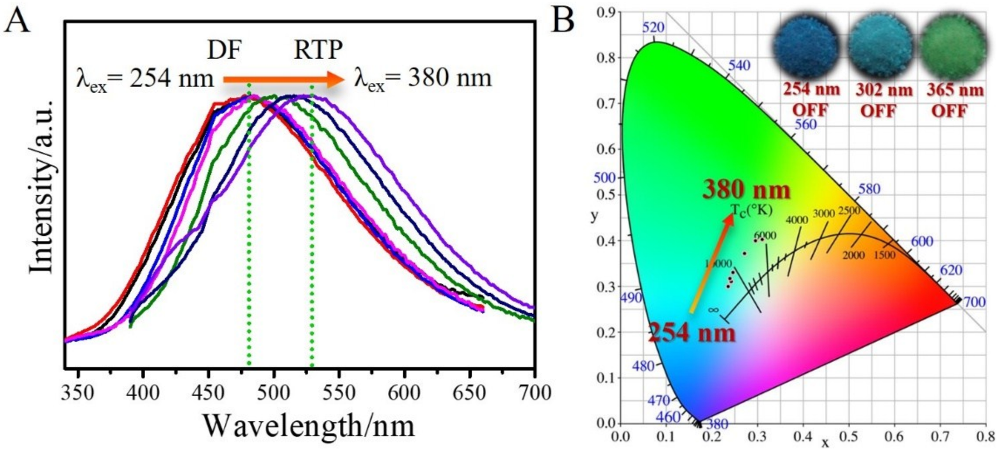

Figure S12. A) Afterglow emission spectra of CDs-3@clay (3,4-pyridinedicarboxylic acid as guest molecules) under different excitation wavelengths. B) CIE coordinate diagram of CDs-3@clay (3,4-pyridinedicarboxylic acid as guest molecules) under different excitation wavelengths.

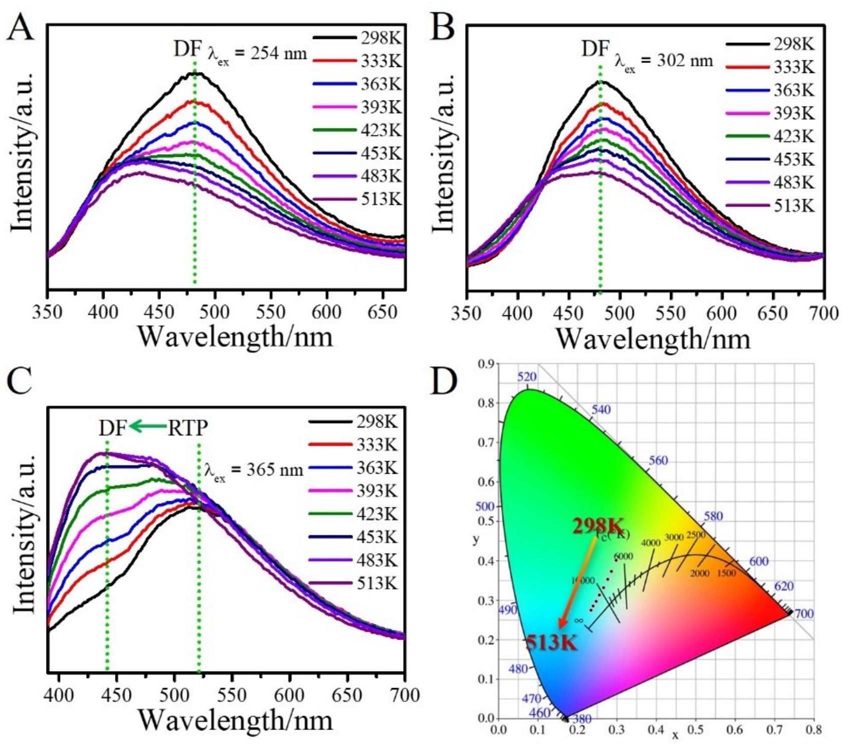

Figure S13. Afterglow emission spectra of CDs-3@clay (3,4-pyridinedicarboxylic acid as guest molecules) at different temperatures under A) 254 nm, B) 302 nm and C) 365 nm excitation. D) CIE coordinate diagram of CDs-3@clay (3,4-pyridinedicarboxylic acid as guest molecules) at different temperatures under 365 nm excitation.

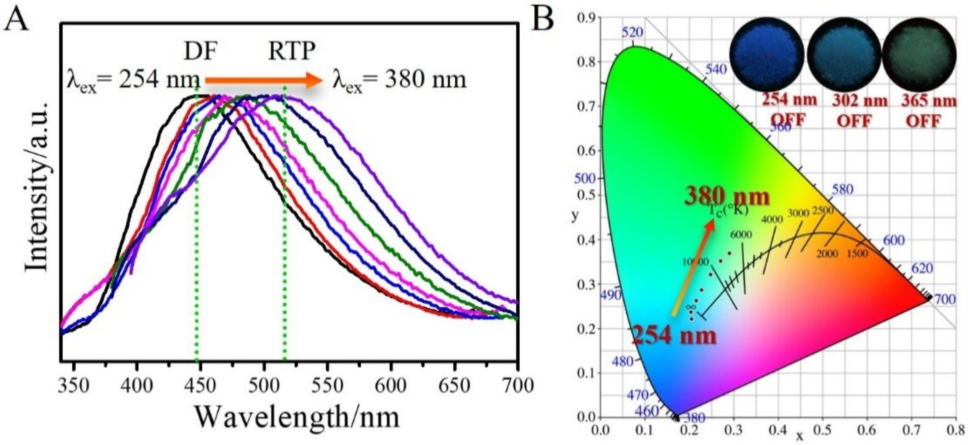

Figure S14. A) Afterglow emission spectra of CDs-5@clay (isophthalic acid as guest molecules) under different excitation wavelengths. B) CIE coordinate diagram of CDs-5@clay (isophthalic acid as guest molecules) under different excitation wavelengths.

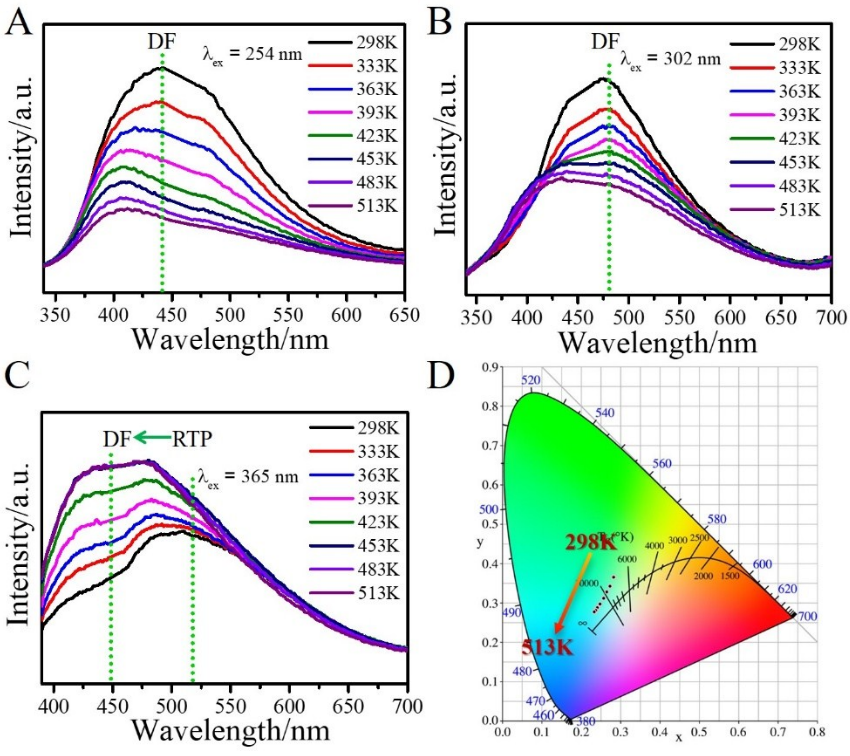

Figure S15. Afterglow emission spectra of CDs-5@clay (isophthalic acid as guest molecules) at different temperatures under A) 254 nm, B) 302 nm and C) 365 nm excitation. D) CIE coordinate diagram of CDs-3@clay CDs-5@clay (isophthalic acid as guest molecules) at different temperatures under 365 nm excitation.

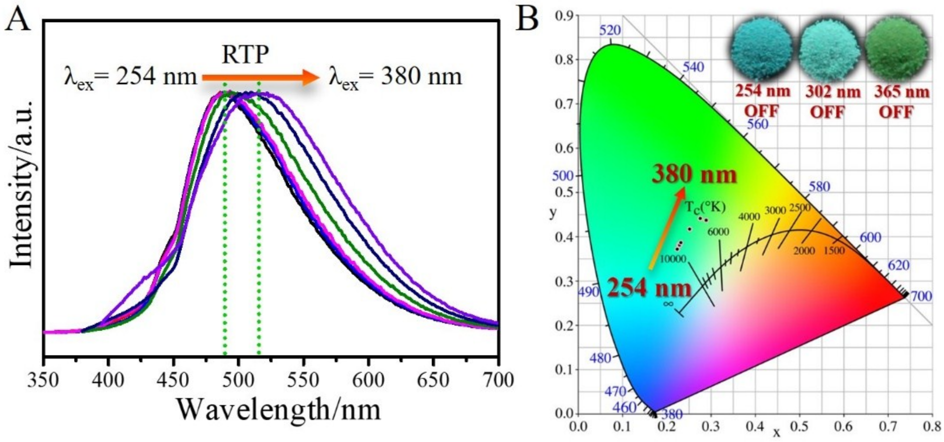

Figure S16. A) Afterglow emission spectra of CDs-6@clay (2,2'-Bipyridine as guest molecules) under different excitation wavelengths. B) CIE coordinate diagram of CDs-6@clay (2,2'-Bipyridine as guest molecules) under different excitation wavelengths.

Table S2. The photophysical characteristics of CDs-6@clay (2,2'-Bipyridine as guest molecules) at the low temperature (77 K) under different excitation wavelengths.

Excitation wavelength	254 nm	280 nm	302 nm	320 nm	340 nm	360 nm	370 nm
Fluorescence	398 nm	398 nm	398 nm	398 nm	398 nm	408 nm	413 nm
Afterglow	482 nm	482 nm	484 nm	484 nm	496 nm	508 nm	513 nm
ΔE_{ST}	0.54 eV	0.54 eV	0.55 eV	0.55 eV	0.62 eV	0.60 eV	0.59 eV

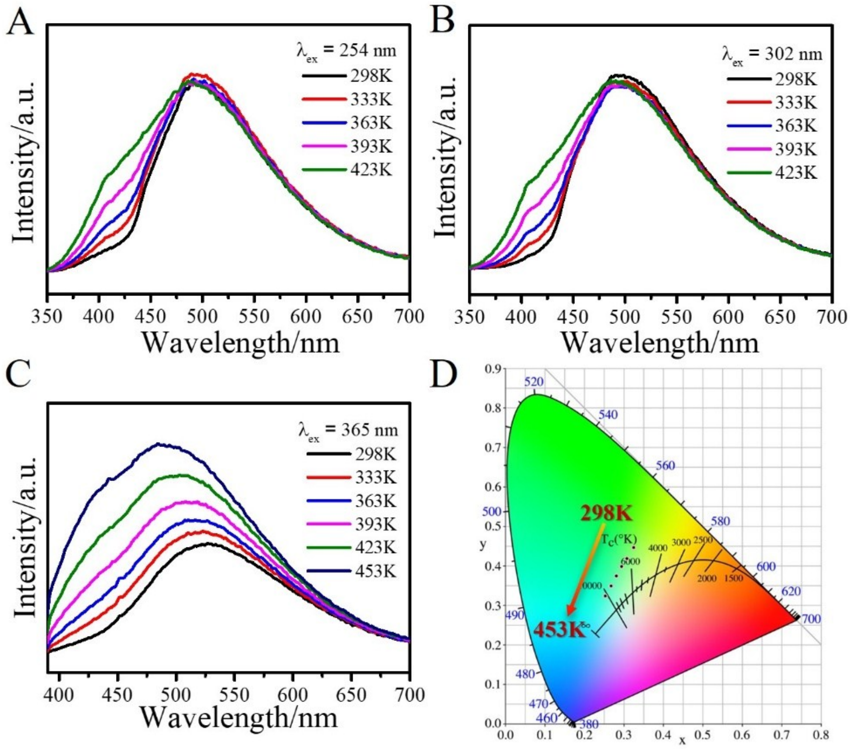

Figure S17. Afterglow emission spectra of CDs-6@clay (2,2'-Bipyridine as guest molecules) at different temperatures under A) 254 nm, B) 302 nm and C) 365 nm excitation. D) CIE coordinate diagram of CDs-3@clay CDs-6@clay (2,2'-Bipyridine as guest molecules) at different temperatures under 365 nm excitation.

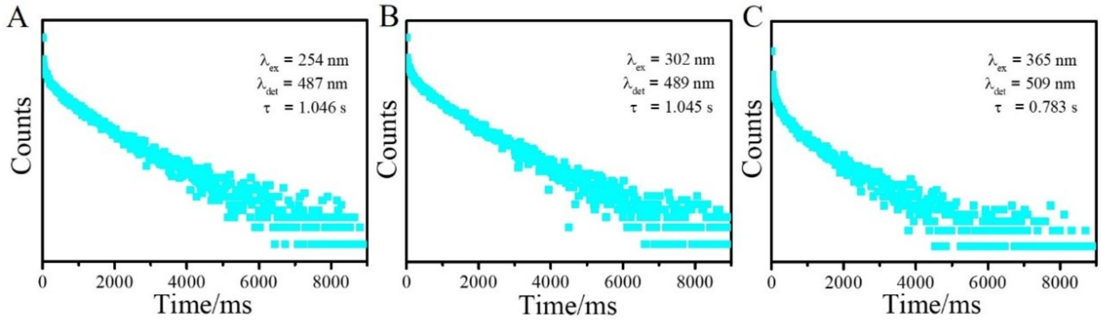

Figure S18. A-C) Afterglow decay curves of CDs-6@clay (2,2'-Bipyridine as guest molecules) under excitation at 254 nm, 302 nm and 365 nm.

Table S3. Afterglow lifetimes of CDs-6@clay (2,2'-Bipyridine as guest molecules) under different excitation wavelengths.

Excitation	τ_1/s	τ_2/s	Average<τ>/s	χ^2

wavelength				
254 nm	0.419 (22.68 %)	1.230 (77.32%)	1.046	1.298
302 nm	0.391 (17.26 %)	1.182 (82.74 %)	1.045	1.378
365 nm	0.197 (26.64 %)	0.996 (73.36 %)	0.783	1.186

References

1. D. Yang, Y. Wang, Y. Wang, Z. Li, H. Li, *ACS Appl. Mater. Interfaces*, **2015,** *7*, 2097.

2. P. Li, Z. Li, H. Li, *Adv. Opt. Mater.*, **2016,** *4*, 156.